Implication of shell quenching in scandium isotopes around N=20*

Rong An (安荣)[1,2,3] Xiang Jiang (蒋翔)[4] Na Tang (唐娜)[1]
Li-Gang Cao (曹李刚)[3,5†] Feng-Shou Zhang (张丰收)[3,5,6‡]

[1]School of Physics, Ningxia University, Yinchuan 750021, China
[2]Guangxi Key Laboratory of Nuclear Physics and Technology, Guangxi Normal University, Guilin 541004, China
[3]Key Laboratory of Beam Technology of Ministry of Education, School of Physics and Astronomy, Beijing Normal University, Beijing 100875, China
[4]College of Physics and Optoelectronic Engineering, Shenzhen University, Shenzhen 518060, China
[5]Key Laboratory of Beam Technology of Ministry of Education, Institute of Radiation Technology, Beijing Academy of Science and Technology, Beijing 100875, China
[6]Center of Theoretical Nuclear Physics, National Laboratory of Heavy Ion Accelerator of Lanzhou, Lanzhou 730000, China

Abstract: Shell closure structures are commonly observed phenomena associated with nuclear charge radii throughout the nuclide chart. Inspired by recent studies demonstrating that the abrupt change can be clearly observed in the charge radii of the scandium isotopic chain across the neutron number N=20, we further review the underlying mechanism of the enlarged charge radii for ^{42}Sc based on the covariant density functional theory. The pairing correlations are tackled by solving the state-dependent Bardeen-Cooper-Schrieffer equations. Meanwhile, the neutron-proton correlation around the Fermi surface derived from the simultaneously unpaired proton and neutron is appropriately considered in describing the systematic evolution of nuclear charge radii. The calculated results suggest that the abrupt increase in charge radii across the N=20 shell closure seems to be improved along the scandium isotopic chain if the strong neutron-proton correlation is properly included.

Keywords: charge radii, shell quenching, relativistic mean field theory, neutron-proton correlations

DOI: 10.1088/1674-1137/adb416 **CSTR:** 32044.14.ChinesePhysicsC.49064105

I. INTRODUCTION

For self-bound complex nuclei systems, quantum shell closure effects are observed in various physical quantities, such as α-decay properties [1−5], nuclear mass evolution [6−9], and the systematic trend of changes in nuclear charge radii [10−13]. A fully filled shell results in a nucleus having relatively stable properties with respect to the adjacent counterparts. Particularly, along a long isotopic chain, the shrinking trend in nuclear charge radii (being the kink phenomenon) can be evidently observed at the fully filled neutron numbers $N = 28$, 50, 82, and 126 [14, 15]. This results in the local minima of proton radii along a long isotopic chain. Meanwhile, imprints of the shell closures at the neutron numbers $N = 14$ and $N = 16$ can be identified in the proton density distributions [16−18]. Therefore, the signature of neutron magicity can be identified from the local variations in nuclear charge radii.

Charge radii of neutron-rich isotopes beyond the neutron-closed shell $N = 28$ appear to increase with similar slopes [19, 20]. Across the traditional neutron magic numbers $N = 20$, the abrupt change in nuclear charge radii unexpectedly disappears in the calcium isotopes. The same scenarios can be encountered in the neighboring Ar [21] and K [22−24] isotopic chains; specifically, only smooth variations are presented in the charge radii. The apparent disappearance of the rapid increase in nuclear charge radii poses a long-standing challenge to nuclear many-body theory across the traditional neutron number $N = 20$. A potentially reduced charge radius of ^{32}Al seems to support an effect of the $N = 20$ shell clos-

Received 23 October 2024; Accepted 10 February 2025; Published online 11 February 2025

* Partly supported by the Open Project of Guangxi Key Laboratory of Nuclear Physics and Nuclear Technology (NLK2023-05), the Central Government Guidance Funds for Local Scientific and Technological Development, China (Guike ZY22096024), the Natural Science Foundation of Ningxia Province, China (2024AAC03015), and the Key Laboratory of Beam Technology of Ministry of Education, China (BEAM2024G04). Xiang Jiang is supported by the National Natural Science Foundation of China (11705118, 12175151), and the Major Project of Basic and Applied Basic Research Foundation of Guangdong Province, China (2021B0301030006). Li-Gang Cao is supported by the National Natural Science Foundation of China (12275025, 11975096), and the Fundamental Research Funds for the Central Universities (2020NTST06). Feng-Shou Zhang is supported by the National Key R&D Program of China (2023YFA1606401) and the National Natural Science Foundation of China (12135004, 11635003, 11961141004, 12047513)

† E-mail: caolg@bnu.edu.cn
‡ E-mail: fszhang@bnu.edu.cn

ure from nuclei size [25]. Recent research reveals that charge radii of neutron deficient ^{40}Sc (3.514±0.025 fm) and ^{41}Sc(3.503±0.020 fm) isotopes can be detected using collinear laser spectroscopy approach [26]. Combining the existing charge radius of ^{42}Sc(3.557±0.014 fm) in Ref. [27], the abrupt increase in charge radii can be observed from ^{41}Sc to ^{42}Sc. Therefore, a pronounced kink phenomenon at the neutron number $N = 20$ can be verified from the aspect of nuclear charge radii in the scandium isotopes.

The undertaken efforts have been devoted to describing the trend of changes in nuclear charge radii, such as the applied empirical formulas ruled by the $A^{1/3}$ or $Z^{1/3}$ law [28, 29], relativistic [30, 31] and non-relativistic [32−34] energy density functionals, and machine learning approaches [35−41]. Here, the microscopic mechanisms cannot be properly captured by the empirical formulas. As suggested in Ref. [26], the charge radius of ^{41}Sc is significantly below the value of ^{42}Sc, and this results in the pronounced kink structure at the neutron number $N = 20$ along the scandium isotopic chain. However, both the *ab initio* and density functional theory (DFT) models cannot reproduce the increasing pattern of charge radii for neutron-deficient scandium isotopes. Nevertheless, as demonstrated in Refs. [42, 43], the local variations in nuclear charge radii cannot be reproduced well at the mean-field level.

The discontinuous variations in nuclear charge radii, such as the shell quenching phenomena, can be described well by incorporating the Casten factor, in which the neutron-proton correlations are derived from the valence neutrons and protons [44−47]. A similar approach that considers the neutron-proton correlations around the Fermi surface in the root-mean-square (rms) charge radii formula has been proposed to describe the fine structure of nuclear size through the covariant density functional theory (CDFT) model. This modified method can reproduce the anomalous behaviors of charge radii along a long isotopic family; however, the odd-even staggering (OES) effect is profoundly overestimated along odd-Z isotopic chains [48, 49]. To resolve this tension, the neutron-proton correlation derived from the simultaneously unpaired neutron and proton around the Fermi surface has been incorporated into the rms charge radii formula [50]. Although the correlation between the simultaneously unpaired neutron and proton has been considered, the calculated charge radius of ^{42}Sc is underestimated. Thus, the neutron-proton correlation cannot be captured adequately for the unpaired nucleons. Therefore, the underlying mechanism should be clarified for a deeper understanding.

For the isotope ^{42}Sc, the last unpaired proton and neutron occupy the $1f_{7/2}$ shell with respect to the relatively stable core ^{40}Ca. The blocking approximation is employed to tackle the unpaired nucleons [50]. For these nucleons with time-reversal symmetry breaking, the unpaired single particle occupations should be tackled appropriately. To further review the underlying mechanism for the enlarged charge radii from ^{41}Sc to ^{42}Sc, the CDFT model is employed in this study. The pairing correlations are properly tackled by solving the state-dependent Bardeen-Cooper-Schrieffer equations [31]. The quadrupole deformation and the neutron-proton pairing correlation around the Fermi surface are incorporated into our discussion. The influence of different occupations of the proton and neutron single particle levels on the charge radius of ^{42}Sc is inspected for the simultaneously unpaired neutron and proton in this study.

The remainder of this paper is organized as follows. In Sec. II, the theoretical framework is briefly presented. In Sec. III, the numerical results and discussion are provided. Finally, Sec. IV summarizes the study.

II. THEORETICAL FRAMEWORK

The covariant density functional theory (CDFT) model has enabled description of various physical phenomena [51−67]. For nonlinear self-consistent Lagrangian density, the effective interactions among nucleons are provided by the exchange of σ, ω, and ρ mesons. The electromagnetic interaction is offered by photons naturally. The effective Lagrangian density is recalled as follows [68]:

$$\begin{aligned}\mathcal{L} = {} & \bar{\psi}[\mathrm{i}\gamma^{\mu}\partial_{\mu} - M - g_{\sigma}\sigma - \gamma^{\mu}(g_{\omega}\omega_{\mu} + g_{\rho}\vec{\tau}\cdot\vec{\rho}_{\mu} + eA_{\mu})]\psi \\ & + \frac{1}{2}\partial^{\mu}\sigma\partial_{\mu}\sigma - \frac{1}{2}m_{\sigma}^{2}\sigma^{2} - \frac{1}{3}g_{2}\sigma^{3} - \frac{1}{4}g_{3}\sigma^{4} \\ & - \frac{1}{4}\Omega^{\mu\nu}\Omega_{\mu\nu} + \frac{1}{2}m_{\omega}^{2}\omega_{\mu}\omega^{\mu} + \frac{1}{4}c_{3}(\omega^{\mu}\omega_{\mu})^{2} - \frac{1}{4}\vec{R}_{\mu\nu}\cdot\vec{R}^{\mu\nu} \\ & + \frac{1}{2}m_{\rho}^{2}\vec{\rho}^{\mu}\cdot\vec{\rho}_{\mu} + \frac{1}{4}d_{3}(\vec{\rho}^{\mu}\vec{\rho}_{\mu})^{2} - \frac{1}{4}F^{\mu\nu}F_{\mu\nu}, \end{aligned} \tag{1}$$

where M is the mass of the nucleon, while m_{σ}, m_{ω}, and m_{ρ} are the masses of the σ, ω, and ρ mesons, respectively. Here, g_{σ}, g_{ω}, g_{ρ}, g_2, g_3, c_3, d_3, and $\mathrm{e}^2/4\pi$ correspond to the coupling constants for σ, ω, and ρ mesons and the photon, respectively.

The Dirac equation with effective fields $S(\mathbf{r})$ and $V(\mathbf{r})$ and Klein-Gordon equations with various mesons sources are derived through the variational principle [68]. To capture the ground-state properties of finite nuclei, the quadrupole deformation parameter β_{20} becomes constrained in the self-consistently iterative process. Therefore, the Hamiltonian formalism can be rewritten as follows:

$$\mathcal{H} = \alpha\cdot\mathbf{p} + V(\mathbf{r}) + \beta[M + S(\mathbf{r})] - \lambda\mathbf{Q}, \tag{2}$$

where λ is the spring constant, and $\mathbf{Q}$ is the intrinsic quadrupole moment operator. Those values of the corres-

ponding quadrupole deformation parameter β_{20} are changed from −0.25 to 0.25 with the interval range of 0.01.

To account for the implications of the observed odd-even oscillations of nuclear charge radii along odd-Z isotopic chains, a modified mean-square charge radii formula has been proposed as follows (in units of fm^2) [50]:

$$R^2_{\rm ch} = \langle r^2_{\rm p}\rangle + 0.7056\ {\rm fm}^2 + \frac{a_0}{\sqrt{A}}\Delta\mathcal{D}\ {\rm fm}^2 + \frac{\delta}{\sqrt{A}}\ {\rm fm}^2. \quad (3)$$

The first term represents the charge distribution of point-like protons, and the second term is owing to the finite size of protons [69]. Here, the quantity of the proton radius assumes values of approximately 0.84 fm [70, 71]. As shown in Eq. (3), the quantity of $|\Delta\mathcal{D}|$ is associated with the difference in Cooper pair condensation between the neutrons and protons [72]. The effective force in the covariant density functional theory is chosen to be the parameter set NL3 [73]. The last term in this expression represents the neutron-proton correlation derived from the simultaneously unpaired neutron and proton. Therefore, the quantity of δ equals zero for even-even, even-odd, and odd-even nuclei. The values of $a_0 = 0.561$ and $\delta = 0.355$ are calibrated by fitting the odd-even oscillation and the inverted parabolic-like shape of charge radii along potassium and calcium isotopes under effective force NL3 [50]. The pairing strength is determined through empirical odd-even mass staggering [74]. As shown in Ref. [50], the pairing strength is chosen as $V_0 = 350$ MeV fm^3 for the effective force NL3 set.

III. RESULTS AND DISCUSSION

The signatures of neutron magic numbers can be reflected through binding energies, nuclear charge radii, excitation energies, and transition probabilities [19, 75, 76]. As in a strongly correlated many-body system, the rapid rise in nuclear charge radii along a long isotopic chain results from different mechanisms, such as the shape-phase transition [77−79] and the shell closure effect [10−13]. The isotopes with neutron magic numbers exhibit relatively stable binding energies, and their proton density distributions exhibit rather smaller variations in comparison with those of neighboring counterparts. In this study, the calculated result suggests that the quadrupole deformation β_{20} for ^{42}Sc is approximately −0.07, resulting in an almost spherical shape. This is in accordance with the value shown in Ref. [80]. The spherical shape has also been presented for ^{41}Sc [50]. Thus, the influence originating from the quadrupole deformation is not adequate in reproducing the abruptly increasing trend of charge radii from ^{41}Sc to ^{42}Sc isotopes. The rapid increase in charge radius can be clearly observed across the ^{41}Sc isotope [26]. However, this profound kink structure at the $N = 20$ fully filled-shell is absent in the neighboring Ca, K, and Ar isotopic chains.

For the Sc isotopic family, the time-reverse symmetry is broken by the last unpaired proton. Generally, the blocking approximation is employed in tackling the occupation of the last unpaired proton and neutron. The occupation numbers of unpaired neutrons and protons are determined by adjusting them to minimize the nuclear binding energy. Therefore, the blocking treatment of the last unpaired neutron and proton is further inspected in the following discussion. However, the quadrupole deformation has an influence on the determination of nuclear charge radii [81]. Therefore, the potential energy curves (PECs) of ^{42}Sc should be depicted for various blocking states. Fig. 1 shows the plot of the PEC of ^{42}Sc as a function of quadrupole deformation β_{20}. For the convenience of discussion, the projection of the angular momentum on the z-axis in the $1d_{3/2}$ ($j_z = 3/2^+$, $j_z = 1/2^+$) and $1f_{7/2}$ ($j_z = 7/2^-$, $j_z = 5/2^-$, $j_z = 3/2^-$, $j_z = 1/2^-$) shells are employed to declare the occupied orbits for the last unpaired proton (π) and neutron (ν), in which the superscripts + and − represent the parity. The last unpaired neutron (ν) locates sequentially at the single particle levels from the $1d_{3/2}$ to $1f_{7/2}$ subshells. As shown in Figs. 1(a) and (b), the $1d_{3/2}$ level is occupied in order by the last unpaired proton. It can be observed that the local minimum in the PEC of ^{42}Sc diverges considerably from the experimental datum. In contrast, for $\nu 1f7/2^-$ ($j_z = 7/2^-$), the calculated result is relatively close to the experimental datum; however, about 7.0 MeV, deviation can be observed.

As shown in Fig. 1(c), the last unpaired proton occupies the $j_z = 7/2^-$ level. The largest binding energy of ^{42}Sc can be obtained if the last unpaired neutron occupies the $j_z = 7/2^-$ level. Here, one can mention that the quadrupole deformation is at the value of $\beta_{20} = -0.07$, resulting in an almost spherical shape. As shown in Figs. 1(d), (e), and (f), the levels $\pi 1f5/2^-$, $\pi 1f3/2^-$, and $\pi 1f1/2^-$ are sequentially occupied by the last unpaired proton. Furthermore, the local minimum energies are almost similar or equivalent for these cases. This is because quadrupole deformation values are extremely close to each other for the corresponding configuration mixing of the last unpaired single particle levels. The $1f7/2^-$ level occupied by the simultaneously unpaired neutron and proton gives rise to the relatively stable ground-state property of ^{42}Sc. Although the configuration combinations through various levels such as $\pi 1f5/2^-$, $\pi 1f3/2^-$, and $\pi 1f1/2^-$ provide similar results, slight deviations can be noted with respect to the case of the $\pi 1f7/2^-$ level occupied by the simultaneously unpaired nucleons.

To facilitate a quantitative comparison, the rms charge radii of ^{42}Sc are plotted in Fig. 2 as a function of quadrupole deformation β_{20} under various configuration mixing occupations of the simultaneously unpaired neut-

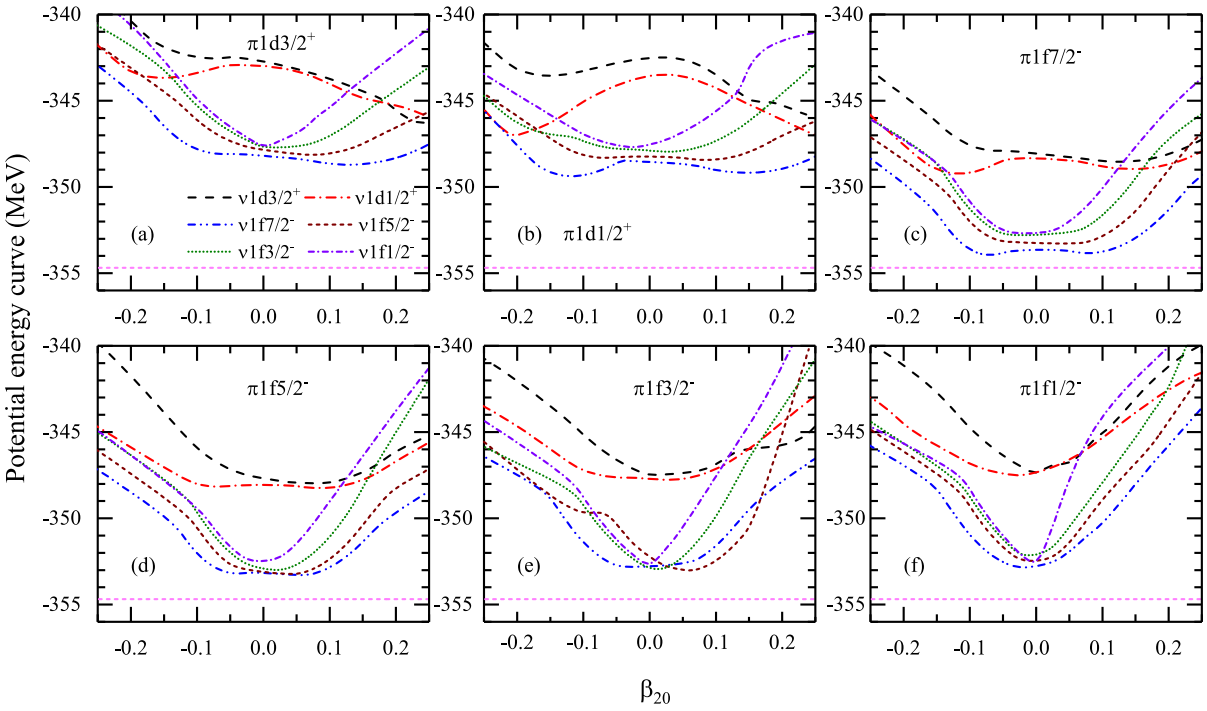

Fig. 1. (color online) Potential energy curve (PEC) of ^{42}Sc as function of quadrupole deformation β_{20} for different configurations of mixing of single particle orbits occupied by the last unpaired nucleons. π and ν denote the last unpaired proton and neutron, respectively, where the components of the angular momentum of the $1d_{3/2}$ ($j_z = 3/2^+$ and $j_z = 1/2^+$) and $1f_{7/2}$ ($j_z = 7/2^-$, $j_z = 5/2^-$, $j_z = 3/2^-$, and $j_z = 1/2^-$) subshells projected on the z-axis are used to denote the occupied states. Experimental data are taken from Ref. [7] and represented by the short horizontal line.

ron and proton. The calculated results can cover the uncertainty range of the charge radius of ^{42}Sc when the last unpaired proton and neutron occupy the $1d_{3/2}$ and $1f_{7/2}$ subshells, respectively. However, for these cases, the ground-state energies are deviated considerably from those of the experiment; in particular, loosely bound states are expected. The same scenarios can be encountered in the configuration where the unpaired proton and neutron occupy the $1f_{7/2}$ and $1d_{3/2}$ subshells, respectively. For the configuration mixing with various levels in the $1f_{7/2}$ subshell, each of these occupied combinations produce a lower value than the experimental one. Therefore, the experimental value cannot be reproduced well through various configuration mixing of the last unpaired neutron and proton.

The signature of local variations can be manifested in nuclear charge radii. To further inspect these discontinuous variations in charge radii for a specific isotopic family, the three-point formula can be recalled as follows [34, 42]:

$$\Delta_r(N,Z) = \frac{1}{2}[2R(N,Z) - R(N-1,Z) - R(N+1,Z)], \quad (4)$$

where $R(N,Z)$ is the rms charge radius for a nucleus with neutron number N and proton number Z. As discussed above, the charge radius of ^{42}Sc cannot be reproduced well by blocking various forms of configuration mixing of the simultaneously unpaired neutron and proton. Meanwhile, combining various occupations of the unpaired single particle levels in our model, the quadrupole deformation parameters β_{20} result in an almost spherical shape. Hence, the abrupt increase in charge radii owing to the shape-phase transition has been excluded in our discussion.

Considering the neutron-proton correlation around the Fermi surface for the simultaneously unpaired neutron and proton, the odd-even staggering (OES) behavior of charge radii can be characterized well along odd-Z isotopic chains. In particular, the OES of charge radii along potassium and copper isotopes can be reproduced well. However, for the scandium isotopic family, the abrupt increase in charge radii from ^{41}Sc to ^{42}Sc cannot be described well in the recently developed model [50]. Thus, the neutron-proton correlation around the Fermi surface is significantly underestimated in our calculations. However, ^{42}Sc can be regarded as a combination of the two valence nucleons and the relatively stable core of ^{40}Ca. To establish the neutron-proton correlation around the Fermi surface, we further redefine the three-point formula along the isotonic chain as follows:

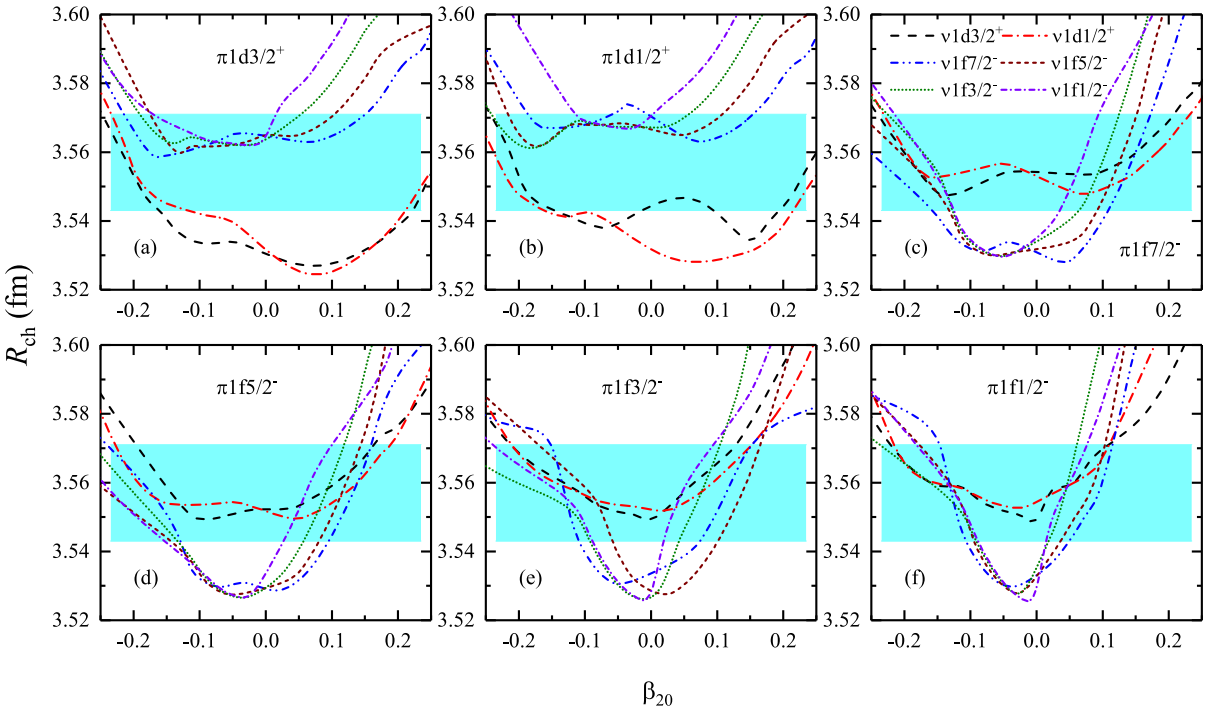

Fig. 2. (color online) Same as Fig. 1 but for the root-mean-square (rms) charge radii. Experimental data are taken from Refs. [26, 27], where the light blue region represents the systematic error band.

$$\Delta(\Delta R_{\rm ch})(N,Z) = \frac{1}{2}[\Delta_r(N,Z) - \Delta_r(N,Z-1) - \Delta_r(N,Z+1)], \tag{5}$$

where the values of $\Delta_r(N,Z)$ can be obtained through Eq. (4).

In Fig. 3, the values of $\Delta(\Delta R_{\rm ch})$ derived from Eq. (5) are used to measure the simultaneously unpaired neutron-proton correlation around the Fermi surface. From this figure, the OES in $\Delta(\Delta R_{\rm ch})$ can be observed with increasing neutron numbers. The calculated results at the neutron numbers $N = 22$, 23, and 24 can reproduce the experimental data well. At the neutron number $N = 21$, the calculated result is apparently underestimated in comparison with the experimental value. Thus, the simultaneously unpaired neutron-proton correlation around the Fermi surface is underestimated significantly for ^{42}Sc, namely the δ value in Eq. (3) is considerably lower. The same scenario can be observed at the neutron number $N = 20$ owing to the overestimated charge radii of ^{40,41}Sc [50]. Therefore, more reliable experimental data are urgently required in the proceeding work.

As shown in Ref. [50], charge radii of ^{40,41}Sc isotopes can be reproduced well with the effective force PK1 in comparison with those obtained by the NL3 set. Therefore, the effective force PK1 [83] is used to depict the trend of changes in charge radii for scandium isotopes in the following discussion. As mentioned above, the neutron-proton correlation seems to be underestimated in Eq. (3). To facilitate the quantitative comparison, charge radii

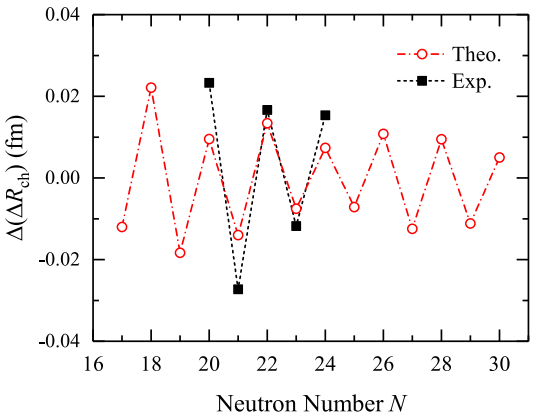

Fig. 3. (color online) Evolution of $\Delta(\Delta R_{\rm ch})$ derived from Eq. (5) according to neutron numbers. Experimental data are taken from Refs. [14, 15, 26, 82].

of the scandium isotopes are shown in Fig. 4. In this figure, the last term in Eq. (3) is sequentially replaced with the $2\delta/\sqrt{A}$ and $4\delta/\sqrt{A}$ modifications. With increasing neutron-proton correlations derived from the simultaneously unpaired neutron and proton, charge radius of ^{42}Sc is enlarged. This causes the significant shrinking trend of charge radii at the neutron number $N = 20$. However, the trend of changes of charge radii cannot be described well at approximately $N = 24$. This may result from the time-reversal symmetry breaking of the unpaired nucleons. As shown in Fig. 4, the value of charge radius for ^{42}Sc remains underestimated. Therefore, more underlying mechanisms should be appropriately considered.

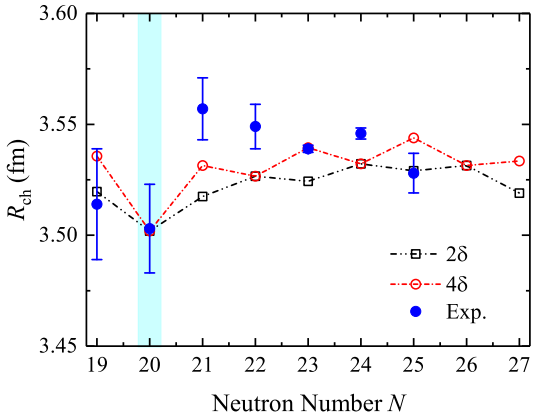

Fig. 4. (color online) Charge radii R_{ch} of scandium isotopes derived from Eq. (3) with 2δ and 4δ modifications as a function of neutron numbers. Experimental data are taken from Refs. [14, 15, 26, 82].

Here, the phenomenological term is used to capture the correlation between the simultaneously unpaired neutron and proton in Eq. (3). The calculated results show that this incorporated term cannot cover the enlargement of charge radii from ^{41}Sc to ^{42}Sc adequately, as shown in Fig. 4. In addition, more underlying mechanisms in treating pairing correlations, such as particle number conservation [61], quadrupole deformation [81], and the appropriate Bogoliubov transformation [51, 84], should be considered. As demonstrated in Refs. [85, 86], the beyond-mean-field approaches play an important role in describing the bulk properties of finite nuclei. As shown in Fig. 1(c), the potential energy curve of ^{42}Sc is relatively soft. Therefore, the beyond-mean-field corrections should be considered in analyzing the enlarged charge radius of ^{42}Sc.

IV. SUMMARY

The signature of nuclear shell structures is generally observed in nuclear charge radii at the traditional neutron magic numbers $N = 28$, 50, 82, and 126. However, as a participant of the traditional neutron magic number $N = 20$, this profound kink structure is absent in Ca, K, and Ar isotopic families. A recent study provides reliable values of charge radii for ^{40}Sc and ^{41}Sc isotopes by employing the laser spectroscopic approach [26]. Considering existing literature [27], the abrupt increase in charge radii can be observed significantly across the $N = 20$ shell closure. This unexpected trend poses a long-standing challenge in theoretical study. This is because ^{42}Sc can be regarded as a combination of the ^{40}Ca core with the simultaneously unpaired neutron and proton in the proton-proton and neutron-neutron channel, respectively.

This study focuses on the following key aspect: the reason behind the unexpected rapid increase in charge radii. The recently developed model that considers the simultaneously unpaired neutron-proton correlation around the Fermi surface has been employed in our discussion [50]. Analyzing various forms of blocking configuration mixing of the simultaneously unpaired neutron and proton, our findings suggest that the influence of quadrupole deformation and blocking configurations on determining the increasing trend of charge radii of ^{42}Sc should be considered properly. Through the values of $\Delta(\Delta R_{ch})$, we can infer that the neutron-proton correlation for the last unpaired nucleons in ^{42}Sc is underestimated significantly. Meanwhile, the overestimated charge radii of ^{40,41}Sc results in the underestimated neutron-proton correlation at the neutron number $N = 20$. As shown in Ref. [87], the overlap between the neutron and proton wave functions can be used to measure the neutron-proton correlation. This seems to provide a microscopic access to capture the correlation between the simultaneously unpaired neutron and proton. Meanwhile, it should be mentioned that the isospin symmetry breaking effect can have an influence on the determination of charge radii [88, 89].

As is well known, nuclear charge radii can be influenced by various mechanisms [90]. A reliable description of charge radii can be used to extract the information about proton size [91]. A highly linear correlation between the difference in charge radii of mirror-pair nuclei and the slope parameter of symmetry energy has been built to pin down the isospin interactions in the equation of state of asymmetric nuclear matter [92−101]. Therefore, the underlying mechanisms should be taken into account properly in describing the nuclear charge radii. Furthermore, more reliable charge radii data are expected in experiments.

References

[1] Z.-S. Ge *et al.*, Phys. Rev. C **98**, 034312 (2018)
[2] Z.-Y. Zhang *et al.*, Phys. Rev. Lett. **122**, 192503 (2019)
[3] S. Tang, Y. Qian, and Z. Ren, Phys. Rev. C **108**, 064303 (2023)
[4] Y. B. Choi *et al.*, Phys. Rev. C **109**, 054310 (2024)
[5] H. Zheng, D. Deng, and Z. Ren, Phys. Rev. C **109**, L011301 (2024)
[6] X. W. Xia *et al.*, At. Data Nucl. Data Tables **121-122**, 1 (2018)
[7] W. J. Huang *et al.*, Chin. Phys. C **45**, 030002 (2021)
[8] K. Y. Zhang *et al.*, At. Data Nucl. Data Tables **144**, 101488 (2022)
[9] P. Guo *et al.*, At. Data Nucl. Data Tables **158**, 101661 (2024)
[10] N. Wang and T. Li, Phys. Rev. C **88**, 011301(R) (2013)
[11] H. Nakada, Phys. Rev. C **100**, 044310 (2019)
[12] U. C. Perera, A. V. Afanasjev, and P. Ring, Phys. Rev. C

104, 064313 (2021)
[13] R. An *et al*., Phys. Rev. C **105**, 014325 (2022)
[14] I. Angeli and K. Marinova, At. Data Nucl. Data Tables **99**, 69 (2013)
[15] T. Li, Y. Luo, and N. Wang, At. Data Nucl. Data Tables **140**, 101440 (2021)
[16] S. Bagchi *et al*., Phys. Lett. B **790**, 251 (2019)
[17] S. J. Novario *et al*., Phys. Rev. C **102**, 051303(R) (2020)
[18] S. Kaur *et al*., Phys. Rev. Lett. **129**, 142502 (2022)
[19] R. F. Garcia Ruiz and A. R. Vernon, Eur. Phys. J. A **56**, 136 (2020)
[20] M. Kortelainen *et al*., Phys. Rev. C **105**, L021303 (2022)
[21] A. Klein *et al*., Nucl. Phys. A **607**, 1 (1996)
[22] F. Touchard *et al*., Phys. Lett. B **108**, 169 (1982)
[23] J. A. Behr *et al*., Phys. Rev. Lett. **79**, 375 (1997)
[24] D. M. Rossi *et al*., Phys. Rev. C **92**, 014305 (2015)
[25] H. Heylen *et al*., Phys. Rev. C **103**, 014318 (2021)
[26] K. König *et al*., Phys. Rev. Lett. **131**, 102501 (2023)
[27] M. Avgoulea *et al*., J. Phys. G **38**, 025104 (2011)
[28] A. Bohr and B. R. Mottelson, *Nuclear structure*, (World Scientific Publishing Co. Pte. Ltd., 1969)
[29] S.-Q. Zhang *et al*., Eur. Phys. J. A **13**, 285 (2002)
[30] P.-W. Zhao *et al*., Phys. Rev. C **82**, 054319 (2010)
[31] L.-S. Geng *et al*., Prog. Theor. Phys. **110**, 921 (2003)
[32] S. Goriely, N. Chamel, and J. M. Pearson, Phys. Rev. C **82**, 035804 (2010)
[33] S. Goriely *et al*., Phys. Rev. Lett. **102**, 242501 (2009)
[34] P. G. Reinhard and W. Nazarewicz, Phys. Rev. C **95**, 064328 (2017)
[35] R. Utama, W.-C. Chen, and J. Piekarewicz, J. Phys. G **43**, 114002 (2016)
[36] X.-X. Dong, R. An, J-.X. Lu *et al*., Phys. Rev. C **105**, 014308 (2022)
[37] J.-Q. Ma and Z.-H. Zhang, Chin. Phys. C **46**, 074105 (2023)
[38] Z.-X. Yang *et al*., Phys. Rev. C **108**, 034315 (2023)
[39] X. Zhang *et al*., Phys. Rev. C **110**, 014316 (2024)
[40] T.-S. Shang *et al*., Phys. Rev. C **110**, 014308 (2024)
[41] A. Jalili and A.-X. Chen, New J. Phys. **26**, 103017 (2024)
[42] R. An, L.-S. Geng, and S.-S. Zhang, Phys. Rev. C **102**, 024307 (2020)
[43] T. Inakura, N. Hinohara, and H. Nakada, Phys. Rev. C **110**, 054315 (2024)
[44] R. F. Casten, D. S. Brenner, and P. E. Haustein, Phys. Rev. Lett. **58**, 658 (1987)
[45] I. Angeli, J. Phys. G **17**, 439 (1991)
[46] Z. Sheng, G. Fan, J. Qian *et al*., Eur. Phys. J. A **51**, 40 (2015)
[47] Z.-Y. Xian, Y. Ya, and R. An, arXiv: 2410.15784 [nucl-th]
[48] R. An *et al*., Chin. Phys. C **46**, 054101 (2022)
[49] R. An *et al*., Chin, Phys. C **46**, 064601 (2020)
[50] R. An *et al*., Phys. Rev. C **109**, 064302 (2024)
[51] J. Meng and P. Ring, Phys. Rev. Lett. **77**, 3963 (1996)
[52] D. Vretenar *et al*., Phys. Rep. **409**, 101 (2005)
[53] L.-G. Cao and Z.-Y. Ma, Eur. Phys. J. A **22**, 189 (2004)
[54] N. Paar *et al*., Phys. Rev. C **67**, 034312 (2003)
[55] S.-G. Zhou, J. Meng, and P. Ring, Phys. Rev. C **68**, 034323 (2003)
[56] N. Paar *et al*., Phys. Rev. C **69**, 054303 (2004)
[57] J. Meng *et al*., Prog. Part. Nucl. Phys. **57**, 470 (2006)
[58] S.-G. Zhou *et al*., Phys. Rev. C **82**, 011301 (2010)
[59] X.-D. Xu *et al*., Phys. Rev. C **92**, 024324 (2015)
[60] X.-X. Sun, J. Zhao, and S.-G. Zhou, Phys. Lett. B **785**, 530 (2018)
[61] R. An *et al*., Chin. Phys. C **44**, 074101 (2020)
[62] X.-X. Sun, J. Zhao, and S.-G. Zhou, Nucl. Phys. A **1003**, 122011 (2020)
[63] K. Wang and B. N. Lu, Commun. Theo. Phys. **74**, 015303 (2022)
[64] Y.-T. Rong *et al*., Phys. Lett. B **840**, 137896 (2023)
[65] Y.-T. Rong, Phys. Rev. C **108**, 054314 (2023)
[66] K.-Y. Zhang, S.-Q. Zhang, and J. Meng, Phys. Rev. C **108**, L041301 (2023)
[67] A. Taninah *et al*., Phys. Rev. C **109**, 024321 (2024)
[68] P. Ring, Y. K. Gambhir, and G. A. Lalazissis, Comput. Phys. Commun. **105**, 77 (1997)
[69] Y. K. Gambhir, P. Ring, and A. Thimet, Ann. Phys. **198**, 132 (1990)
[70] E. Tiesinga *et al*., Rev. Mod. Phys. **93**, 025010 (2021)
[71] Y. H. Lin *et al*., Phys. Rev. Lett. **128**, 052002 (2022)
[72] G. G. Dussel *et al*., Phys. Rev. C **76**, 011302(R) (2007)
[73] G. A. Lalazissis, J. König, and P. Ring, Phys. Rev. C **55**, 540 (1997)
[74] M. Bender *et al*., Eur. Phys. J. A **8**, 59 (2000)
[75] O. Sorlin and M. G. Porquet, Prog. Part. Nucl. Phys. **61**, 602 (2008)
[76] I. Angeli and K. P. Marinova, J. Phys. G **42**, 055108 (2015)
[77] K. Heyde and J. L. Wood, Rev. Mod. Phys. **83**, 1467 (2011)
[78] T. Togashi *et al*., Phys. Rev. Lett. **117**, 172502 (2016)
[79] R. An *et al*., Commun. Theo. Phys. **75**, 035301 (2023)
[80] P. Möller *et al*., At. Data Nucl. Data Tables **109-110**, 1 (2016)
[81] X. Y. Zhang, Z. M. Niu, W. Sun *et al*., Phys. Rev. C **108**, 024310 (2023)
[82] Á. Koszorús *et al*., Nat. Phys. **17**, 439 (1999), [Erratum: Nat. Phys. **17**, 539 (2021)]
[83] W.-H. Long, J. Meng, N. VanGiai *et al*., Phys. Rev. C **69**, 034319 (2004)
[84] J. Meng, Nucl. Phys. A **635**, 3 (1998)
[85] J.-M. Yao *et al*., Phys. Rev. C **84**, 024306 (2011)
[86] K.-Q. Lu *et al*., Phys. Rev. C **91**, 027304 (2015)
[87] G.-A. Miller, A. Beck, S. May-Tal Beck *et al*., Phys. Lett. B **793**, 360 (2019)
[88] T. Naito, G. Colò, H.-Z. Liang *et al*., Phys. Rev. C **105**, L021304 (2022)
[89] T. Naito, X. Roca-Maza, G. Colò *et al*., Phys. Rev. C **106**, L061306 (2022)
[90] S. Geldhof *et al*., Phys. Rev. Lett. **128**, 152501 (2022)
[91] J.-C. Zhang *et al*., Sci. Bull. **69**, 1647 (2024)
[92] B. A. Brown, Phys. Rev. Lett. **119**, 122502 (2017)
[93] J. Yang and J. Piekarewicz, Phys. Rev. C **97**, 014314 (2018)
[94] B. A. Brown *et al*., Phys. Rev. Res. **2**, 022035(R) (2020)
[95] J.-Y. Xu *et al*., Phys. Lett. B **833**, 137333 (2022)
[96] S. V. Pineda *et al*., Phys. Rev. Lett. **127**, 182503 (2021)
[97] S. J. Novario *et al*., Phys. Rev. Lett. **130**, 032501 (2023)
[98] R. An *et al*., Nucl. Sci. Tech. **34**, 119 (2023)
[99] R. An *et al*., Nucl. Sci. Tech. **35**, 182 (2024)
[100] P. Bano *et al*., Phys. Rev. C **108**, 015802 (2023)
[101] K. König *et al*., Phys. Rev. Lett. **132**, 162502 (2024)